Differential uplift of three Pliocene sea level indicators in southern Argentina driven by upwelling asthenosphere through the Patagonian slab window

Lamont-Doherty Earth Observatory
COLUMBIA UNIVERSITY | EARTH INSTITUTE

Andrew, Hollyday[1], Jacqueline Austermann[1], Andrew Lloyd[1], Mark Hoggard[1,2], Fred Richards[3], Alessio Rovere[4]

1. Department of Earth & Environmental Science, Columbia University | Lamont-Doherty Earth Observatory, Palisades, NY
2. Department of Earth & Planetary Sciences, Harvard University, Cambridge, MA
3. Department of Earth Science & Engineering, Imperial College London, London, UK
4. MARUM, University of Bremen, Bremen, Germany

Pliocene sea level indicators & Patagonia slab window

Uplifted marine bivalve and mollusk shell beds deposited during the early Pliocene record relative sea level during a time when temperatures and CO_2 were higher than today (e.g., Pagani et al., 2010). These deposits occur at strikingly differentially uplifted elevations along a near-longitudinal transect (Fig., below). In this study, we use geodynamic models of mantle flow to constrain how changes in dynamic topography have differentially uplifted these sites with the ultimate goal of estimating the global mean sea level in the early Pliocene

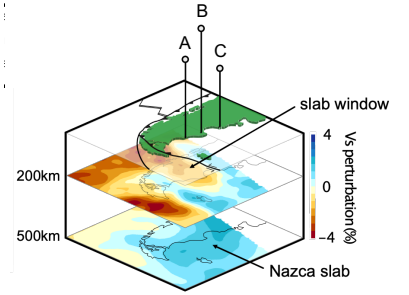

Site	Elevation	SIS age
A	65 - 75 m	5.15 ± 0.35 Ma
B	170 - 185 m	5.1 ± 0.30 Ma
C	34.5 - 38.9 m	4.98 ± 0.23 Ma

Beginning ~18 Ma the Chile Rise spreading ridge began subducting beneath the South American plate (Breitsprecher & Thorkelson, 2009). As the ridge migrated north, a gap formed where the Nazca slab had previously been subducting, allowing underlying hot aesthenosphere to flow into the mantle wedge. Both the slow-velocity slab window (200 km) and the fast-velocity Nazca slab (500 km) have been imaged using adjoint seismic tomography (Lloyd et al., 2020) and indicate interplay between upwelling and downwelling mantle flow.

Hypothesis:

The combination of the previously subducted Nazca slab and asthenospheric upwelling through the overlying Patagonian slab window have produced short wavelength changes in dynamic topography that explain a sharp gradient in the elevations of Pliocene sea level indicators along the eastern coast of Argentina.

Tomography-based Earth models

Seismic velocity to temperature

(Richard et al, 2020; Steinberger, 2016; Yamauchi & Takei, 2016)

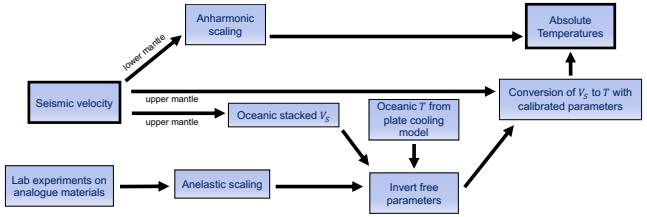

Temperature models

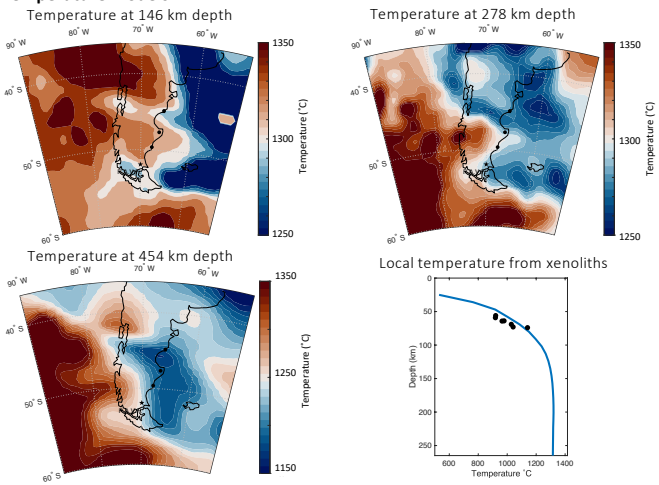

Pressure and temperature calculations (Nickel & Green, 1985; Taylor, 1998) exploit available major element compositions from olivine, orthopyroxene, clinopyroxene, and garnet hosted in high-temperature (>970 ˚C) peridotites, garnet-spinel harzburgites, and garnet lherzolites from the Pali-Aike Volcanic Field (see maps). These independent temperatures agree with the tomography-based Earth model (lower right panel).

Mantle convection simulations & dynamic topography change

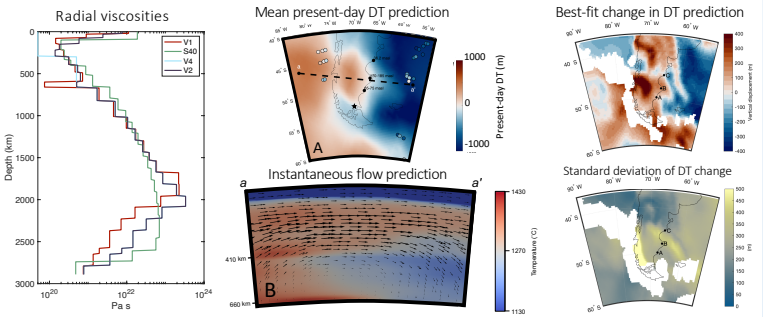

The suite of dynamic topography results from 11 postprocessing plate correction models for the 36 model configurations consisting of eight unique Earth models allows us to isolate specific model runs that fit the observed elevation gradient best. While model runs fit the southern two shoreline sites well, the northernmost site remains poorly fit. To better understand the full range of possible geodynamic processes at play, we plan to broaden the Earth model suite to include more tomography models of the lower mantle and the range of radial viscosities.

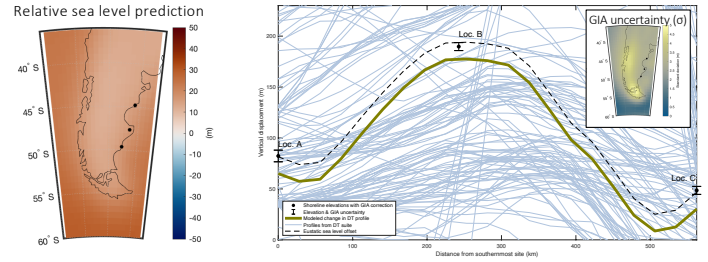

References

Breitsprecher & Thorkelson (2009). Neogene kinematic history of Nazca–Antarctic–Phoenix slab windows beneath Patagonia and the Antarctic Peninsula. *Tectonophysics.*

Lloyd, et al. (2020). Seismic Structure of the Antarctic Upper Mantle Imaged with Adjoint Tomography. *J. Geophys. Res.: Solid Earth.*

Nickel & Green (1985). Empirical geothermobarometry for garnet peridotites and implications for the nature of the lithosphere, kimberlites and diamonds. *Earth and Planet. Sci. Let.*

Pagani, et al. (2010). High Earth-system climate sensitivity determined from Pliocene carbon dioxide concentrations. *Nat. Geo.*

Richards et al. (2020). Quantifying the Relationship Between Short-Wavelength Dynamic Topography and Thermomechanical Structure of the Upper Mantle Using Calibrated Parameterization of Anelasticity. *J. Geophys. Res.: Solid Earth.*

Steinberger (2016). Topography caused by mantle density variations: Observation-based estimates and models derived from tomography and lithosphere thickness. *Geophys. J. Int.*

Taylor (1998). An experimental test of some geothermometer and geobarometer formulations for upper mantle peridotites with application to the ther-mobarometry of fertile lherzolite and garnet websterite. *Neues Jahrbuch Für Mineralogie - Abhandlungen.*

Yamauchi & Takei (2016). Polycrystal anelasticity at near-solidus temperatures. *J. Geophys. Res.: Solid Earth.*